IL NUOVO CIMENTO Vol. 29 C, N. 3 Maggio-Giugno 2006
DOI 10.1393/ncc/i2006-10003-5

Optical and electronic properties of manganese thiophosphate and H_2T_4 porphyrin metal complexes films

V. Grasso(1)(2), T. Quattrone(2)(*), L. Silipigni(1)(2), G. De Luca(3), L. Monsú Scolaro(3) and G. Salvato(4)

(1) *Dipartimento di Fisica della Materia e Tecnologie Fisiche Avanzate, Università di Messina Salita Sperone 31, I-98166 Messina, Italy*
(2) *Centro Siciliano per le Ricerche Atmosferiche e di Fisica dell'Ambiente Salita Sperone 31, I-98166 Messina, Italy*
(3) *Dipartimento di Chimica Inorganica, Chimica Analitica e Chimica Fisica Università di Messina - Salita Sperone 31, I-98166 Messina, Italy*
(4) *Istituto per i Processi Chimico-Fisici del CNR, Sezione di Messina - Via La Farina 237 I-98123 Messina, Italy*

(ricevuto il 4 Gennaio 2006; approvato il 16 Febbraio 2006; pubblicato online il 21 Giugno 2006)

Summary. — Films of manganese thiophosphate ($MnPS_3$) and Mn(III)T_4 porphyrin, obtained from a reaction of a colloidal suspension of $MnPS_3$ nanosheets with an aqueous solution of the porphyrin, have been investigated by means of optical absorption and X-ray photoemission spectroscopies. Our attention is turned to the (300–850) nm range and to the C and N 1*s*, Mn, P, S and Cl 2*p* and Mn 3*p* core regions. The analysis of the resulting spectra and their comparison with those reported for the original compounds has allowed us to obtain information both about the interaction between $MnPS_3$ and Mn(III)T_4 and the effects produced by the porphyrin metallation.

PACS 79.60.-i – Photoemission and photoelectron spectra.
PACS 78.66.Sq – Composite materials.
PACS 78.67.-n – Optical properties of low-dimensional, mesoscopic, and nanoscale materials and structures.
PACS 78.20.-e – Optical properties of bulk materials and thin films.

1. – Introduction

Since the immobilization of organic molecules within inorganic hosts has appeared as a very promising approach to design new systems with possible applications in optoelectronics, photonics and energetics, the interest in the inorganic $MnPS_3$ matrix has

(*) E-mail: teresa.quattrone@unime.it

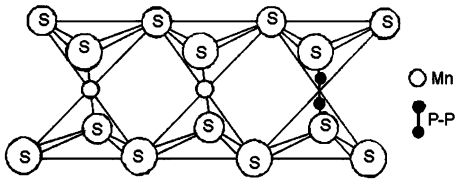

Fig. 1. – Structure of the minimal sandwich $[SMn_{2/3}(P_2)_{1/3}S]$ in $MnPS_3$.

grown during recent years. This attention stems from the $MnPS_3$ ability to form, after exfoliation to single layers through successive intercalation of K^+ and Li^+ cations, $Li_{2x}Mn_{1-x}PS_3$ films which are capable of intercalating organic species [1,2]. In this way it is possible to obtain hybrid films of organic-inorganic nanocomposites by exchanging the lithium ions for the given organic guest species, through an ion-exchange intercalation. Figure 1 shows the structure of the minimal sandwich $[SMn_{2/3}(P_2)_{1/3}S]$, whose succession along the crystallographic c-axis gives rise to the crystalline structure of $MnPS_3$: two honeycomb sulphur atom sheets in which octahedral interstitial sites are occupied for a third by the P-P pairs and for the remaining two thirds by the metal cations. These single sandwiches $[SMn_{2/3}(P_2)_{1/3}S]$ are held together by weak van der Waals forces. The intercalation of cationic species in $MnPS_3$ is made possible by the departure of Mn^{2+} intralayer cations from the host matrix to counterbalance the electrical charge of the guest entering the interlayer spaces. The $MnPS_3$ was found to be a suitable host for nonlinear optical dyes [3, 4] and photochromic molecules [5] because of its optical transparency. Moreover upon intercalation $MnPS_3$ can exhibit spontaneous magnetization at low temperature opening the possibility to design multi-functional materials [6, 7].

Recently, a water-soluble cationic dye, the meso-tetrakis (N-methylpyridinium-4-yl) porphyrin labeled as H_2T_4, has been intercalated into $MnPS_3$ affording a novel hybrid organic-inorganic composite film [8]. The interaction between the guest species and the host matrix causes a strong flattening of the porphyrin between the layers as evidenced by a relevant bathochromic shift of the Soret band, one of the main absorption features of the porphyrin. Since the spectral properties of this dye can be also modified by metal coordination we have focused our attention on its manganese(III) complex (MnT_4). In this compound the metal ion is coordinated into the center of the macrocyclic ring. In the neutral form of this tetracationic metallo-porphyrin, four Cl^- anions neutralize the four positively charged N-methyl-4-pyridyl groups and one is directly coordinated to the central manganese ion (see fig. 2).

It is known that Mn(III) porphyrins have a square-pyramidal geometry with the metal ion displaced out of the porphyrin plane [9] because of the electrostatic repulsion between the positively charged substituents and the metal ion. In homogeneous aqueous solution at pH 6.8 MnT_4 exists in a monomeric form [10] and has been utilized as spectroscopic probe for nucleic acids [11] or as potential magnetic resonance imaging (MRI) contrast agents [12]. A common feature of porphyrins is the planarity of the central core due to the presence of an extended π-conjugated aromatic system. In particular, MnT_4 presents nonlinear optical properties such as intensity dependent refraction index and/or nonlinear absorption whose magnitude and time response also depend upon the environment [13]. This metalloporphyrin is hydrophilic and widely used as catalyst in the oxidation of hydrocarbons [9,14] and as model for cytochrome P-450 [15]. Aggregation phenomena play a significant role in porphyrin chemistry since many of their physico-chemical properties,

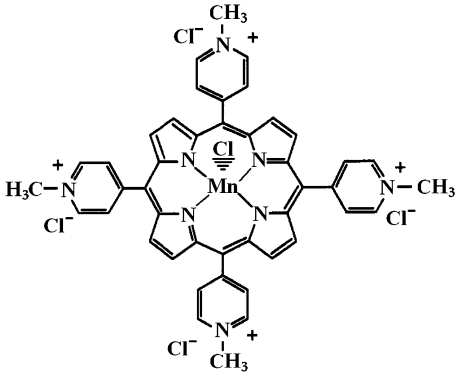

Fig. 2. – Structural representation of the MnT_4 porphyrin.

e.g., the UV-Vis absorption spectra or the fluorescence emission, are strongly modulated by the aggregation state. In this respect, microheterogeneous systems may force porphyrin aggregation. Their propensity to aggregate depends on the presence and the type of metal ion, the protonation state, the nature of substituents, the environmental characteristics and so on. For example aggregation of water-soluble charged porphyrins on polymeric matrices bearing opposite charges is in principle a simple strategy for building tailored supramolecular species [16]. On these bases, the occurrence of an electrostatic attractive interaction between the $Mn(III)T_4$ cationic porphyrin and the negatively charged $Mn_{1-x}PS_3$ sheets of the exfoliated $Li_{2x}Mn_{1-x}PS_3$ compound can be expected. Here we describe our results obtained by performing X-ray diffraction (XRD), optical absorption and X-ray photoemission spectra (XPS) on $MnT_4/Li_{2x}Mn_{1-x}PS_3$ films. In order to point out the role of this interaction on the $MnPS_3$ electronic structure and the metallation of H_2T_4 porphyrin we have also compared our results with $MnPS_3$ and H_2T_4.

2. – Experimental set-up

MnT_4 porphyrin was purchased from MidCentury Chemical Co. as chloride salt and used without further purification. The concentration of the aqueous stock solution of this porphyrin was determined to be 600 μM from UV-Vis absorption measurements ($\epsilon_{463\mathrm{nm}} = 0.92 \times 10^5 \mathrm{M}^{-1}\mathrm{cm}^{-1}$ [12]). The colloidal suspension of the exfoliated $MnPS_3$ nanosheets as $Li_{2x}Mn_{1-x}PS_3$ has been obtained through the same procedure adopted by Silipigni *et al.* [17] starting from a stoichiometric mixture of Mn, P and S of high purity and then intercalating the resulting $MnPS_3$ powders by means of an ion-exchange reaction, first with potassium ions and subsequently with lithium ions. The formation of $MnPS_3$, $K_{2x}Mn_{1-x}PS_3$ and $Li_{2x}Mn_{1-x}PS_3$ was ascertained by XRD measurements. The $MnT_4/Li_{2x}Mn_{1-x}PS_3$ composite films have been prepared starting from an aqueous solution of the MnT_4 porphyrin and a colloidal suspension of $MnPS_3$ nanosheets. In a typical procedure, MnT_4 stock solution was added dropwise under stirring, at room temperature and in the dark to the colloidal suspension up to complete precipitation. The brown precipitate was then collected and washed three times with doubly distilled water. Few drops of the aqueous suspension of the nanocomposite material and of the stock porphyrin solution were casted both onto glass slides and XPS sample holders and allowed to dry in dust-free air for at least two days.

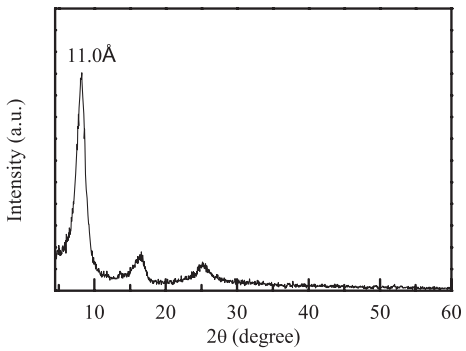

Fig. 3. – XRD pattern for the $MnT_4/Li_{2x}Mn_{1-x}PS_3$ film.

XRD patterns were recorded in the $5° \leq 2\theta \leq 60°$ range with a Philips Analytics diffractometer model PW3710 using the Cu-Kα radiation (1.54 Å). The samples were examined as thin films deposited onto glass slides.

XPS measurements were conducted with a VG Scientific photoelectron spectrometer with an unmonochromatized Al Kα radiation (hν = 1486.6 eV) as the X-ray source. The samples were examined as thin films obtaining a good electrical contact with the spectrometer. Indeed the $MnPS_3$ compound was analyzed as pressed powder pellets. The XPS spectra were obtained at room temperature and typically the operating pressure in the analysis chamber was in the 10^{-9} torr range. The carbon C 1*s* line at 285.0 eV was used as a reference for the determination of the core-level peak binding energies. For each sample a survey scan was recorded with a pass-energy of 50 eV followed by high resolution spectra (at a pass-energy of 20 eV) of individual elements. The XPS spectra, at which a Shirley-type inelastic background has been removed, have been analyzed by means of a least-square fitting procedure using as a model peak a Gaussian-Lorentzian cross-product function. The resulting best fits are shown in figs. 5-8 with a solid line, while the dashed lines are the component bands and the open circles the experimental data.

Absorption measurements were performed at room temperature onto thin films of nanocomposite and MnT_4 with a Perkin-Elmer double-beam UV-Vis spectrophotometer, model Lambda 2. Unpolarized light struck the film surface at normal incidence. The analyzed films were deposited onto glass slides.

3. – Results and discussion

The XRD pattern of the $MnT_4/Li_{2x}Mn_{1-x}PS_3$ films, reported in fig. 3, shows that crystallographically well-ordered structures are obtained with (00*l*) harmonics corresponding to a primary repeat unit (*d* spacing) of 11.0Å. This fact suggests a preferential orientation of the thin film with the sheet stacking parallel to the glass substrate. The difference of 4.5 Å from the corresponding 6.5Å interlayer distance for the original $MnPS_3$ host [2] is in accord with the expected size of the porphyrin ring lying parallel to the $MnPS_3$ layers. The extra structure at about 25.1 Å is due to the substrate. Figure 4 displays the UV-Vis spectra of the $MnT_4/Li_{2x}Mn_{1-x}PS_3$(dashed line) and MnT_4 (solid line) films. In the inset the region between 300 and 450 nm in the MnT_4 film is amplified. The absorption spectrum of MnT_4 porphyrin is similar to that obtained in solution: a

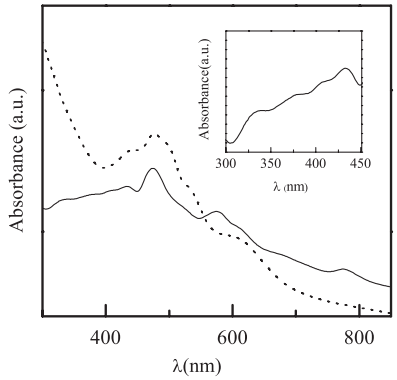

Fig. 4. – UV-Vis spectra of the $MnT_4/Li_{2x}Mn_{1-x}PS_3$ (dashed line) and MnT_4 (solid line) films deposited onto glass substrates.

split Soret band composed of broad overlapping peaks between 450 and 300 nm and a ring-to-metal charge transfer band at about 473 nm, two bands in the visible region located at about 575 and 608 nm corresponding to the Q bands and two bands with weak intensities in the near-infrared region. The interaction of MnT_4 with the $Li_{2x}Mn_{1-x}PS_3$ exfoliated compound causes changes in the absorption spectrum (dashed line) both in the (300–500) nm Soret band and (500–700) nm Q band regions: the Soret band undergoes a bathochromic shift at about 476 nm with hypochromicity while a new band appears around 493 nm. While the small observed red shift of the Soret band ($\Delta\lambda = +3$ nm) seems to indicate that some porphyrin is adsorbed on the external surface of the inorganic matrix, the new structure which is red shifted of about 20 nm with respect to the original Soret band suggests that some porphyrin is intercalated between the inorganic layers. The smaller extent of bathochromic shift observed in the present case with respect to the intercalated H_2T_4 (20 *vs.* 69 nm) [8] could be ascribed to a reduced flattening of the metal derivative with respect to the free base porphyrin. The presence of axial ligands coordinated to the metal center (chloride) probably hinders the close approach of the porphyrin plane to the nanosheets, leaving the N-methyl-4-pyridyl substituents groups more free to rotate.The overlapping peaks visible in the (300–450) nm interval are almost completely merged into a broad structure at about 445 nm. With respect to the Q band region the shoulder is no more weakly resolved and the more intense band is red shifted to around 596 nm.

In figs. 5-8 we report the XPS spectra of the C 1*s*, N 1*s*, Mn 2*p*, P 2*p*, S 2*p*, Mn 3*p*, Li 1*s* and Cl 2*p* core levels for the $MnT_4/Li_{2x}Mn_{1-x}PS_3$ film. Table I lists the core level binding energy positions derived from the fitting procedure taking the C 1*s* binding energy of 285.0 eV as reference for $MnT_4/Li_{2x}Mn_{1-x}PS_3$, MnT_4 and $MnPS_3$. The C 1*s* core level XPS spectrum in the $MnT_4/Li_{2x}Mn_{1-x}PS_3$ film is shown in fig. 5: as observed in the $H_2T_4/Li_{2x}Mn_{1-x}PS_3$ nanocomposite film [8], it exhibits an asymmetric peak positioned at about 285.0 eV with a full width half maximum (FWHM) of 2.3 eV followed by a tail at the higher binding energy side. The tail can be resolved into a weak structure at about 287.9 eV which can be assigned, in analogy to the tetraphenylporphyrin H_2TPP and its copper derivatives [18] and $H_2T_4/Li_{2x}Mn_{1-x}PS_3$ nanocomposite film [8], to a shake-up satellite. Remembering that the FWHM value for a single type of carbon atoms is of 1.06 eV [18], we can safely assign the observed C 1*s* peak to the different carbon atoms

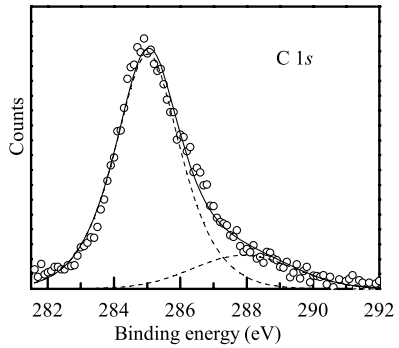

Fig. 5. – C 1*s* core-level XPS spectrum in the $MnT_4/Li_{2x}Mn_{1-x}PS_3$ films.

present in the $MnT_4/Li_{2x}Mn_{1-x}PS_3$ film, whose binding energies are very similar each other.

Figure 6 displays the XPS spectrum of the N 1*s* core level in the MnT_4 film (see section *a*) and in the $MnT_4/Li_{2x}Mn_{1-x}PS_3$ film (see section *b*). In particular fig. 6a shows the effects of the metal coordination on the porphyrin. A comparison between the N 1*s* core-level XPS spectra in the metalloporphyrin and the free-base one (reported in the inset) confirms that the replacement of the free-base protons by a manganese (III) ion makes the four nitrogen atoms of the porphyrin ring equivalent. Consequently, the two peaks observed in the H_2T_4 film at about 398.9 and 401.1 eV, relative to the aza and pyrrole nitrogen atoms in the macrocycle core, respectively, collapse into a single metallonitrogen peak around 402.2 eV. The observed increase in binding energy is likely a consequence of the donation of σ-electron density of porphyrin to the manganese ion through the nitrogen atoms in order to reduce the metal's net positive charge [19]. The other XPS peak at 399.1 eV can be assigned to the four N-methyl-pyridinium nitrogen atoms on the meso substituent groups whose XPS peak is observed at 399.8 eV in the H_2T_4 film. The present data seem to suggest that these latter nitrogen atoms are not in a cationic state probably because the positively charged N-methyl-pyridinium groups of MnT_4 are interacting strongly with their chloride counterion. The peak area ratio of core versus substituent groups nitrogen atoms is 1.0 as expected.

Figure 6b reports the XPS spectrum of the N 1*s* core level in the $MnT_4/Li_{2x}Mn_{1-x}PS_3$ film. A comparison of this spectrum with that of the previously discussed MnT_4 film

TABLE I. – *Core level binding energy values in the $MnT_4/Li_{2x}Mn_{1-x}PS_3$ nanocomposite, $MnPS_3$ and MnT_4 referred to the C 1s line (*285.0 *eV).*

Core-levels	$MnPS_3$	$MnT_4/Li_{2x}Mn_{1-x}PS_3$	MnT_4
S 2*p*	162.4 163.4	162.1 163.1	
P 2*p*	132.9	132.0 133.1	
Mn 2*p*	641.9 653.8	641.6 653.2	641.5 653.1
Mn 3*p*	48.8	48.5	
N 1*s*		399.1 402.0	399.1 402.2
Li 1*s*		55.6	
Cl 2*p*		198.8 200.7	197.9 199.7 198.8 200.7

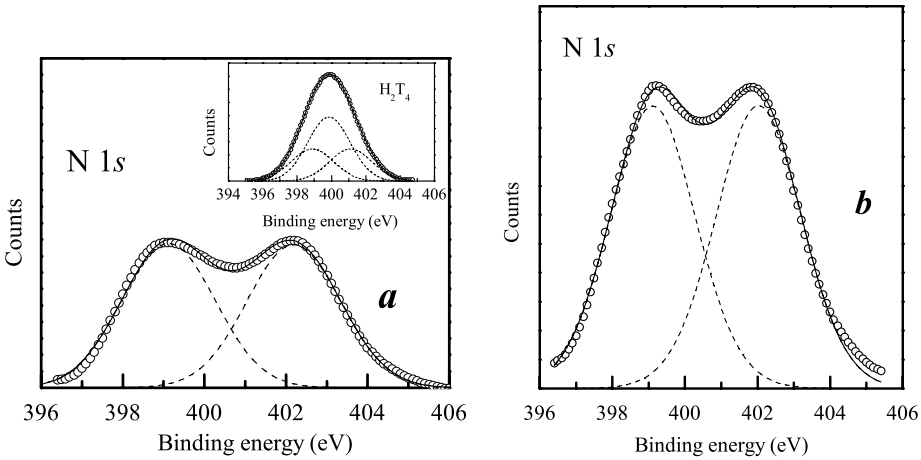

Fig. 6. – N 1s core-level XPS spectrum in the MnT_4 film (see section a) and in the $MnT_4/Li_{2x}Mn_{1-x}PS_3$ film (see section b); the inset displays the XPS spectrum of the same core level observed in the H_2T_4 film [8] for comparison.

(see fig. 6a) suggests that the interaction with the exfoliated manganese thiophosphate does not cause remarkable changes in the binding energy positions: both spectra can be described by two Gaussian-Lorentzian bands having 1:1 ratios and located at the same binding energies within the experimental error.

The Mn 2p core level XPS spectrum of the MnT_4 film is illustrated in fig. 7: it consists of a well-resolved doublet with a binding energy separation of about 11.6 eV for the $2p_{3/2}$ and $2p_{1/2}$ spin-orbit components. This spin-orbit splitting is in agreement with the values observed in other manganese compounds [20]. Moreover the Mn $2p_{3/2}$ core level is located at a binding energy which is greater than in the Mn metal but close to the binding energy observed in other compounds where the metal is present as a trivalent cation [20]. This fact confirms that in the MnT_4 film manganese is in a 3^+ formal oxidation state in agreement with the literature [11]. Like in $MnPS_3$ and in other transition metal thiophosphates [21] each spin-orbit component is accompanied by a shake-up type satellite structure at higher binding energy. When the MnT_4 porphyrin

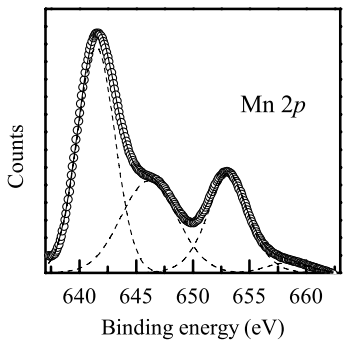

Fig. 7. – Mn 2p core-level XPS spectrum in the MnT_4 films.

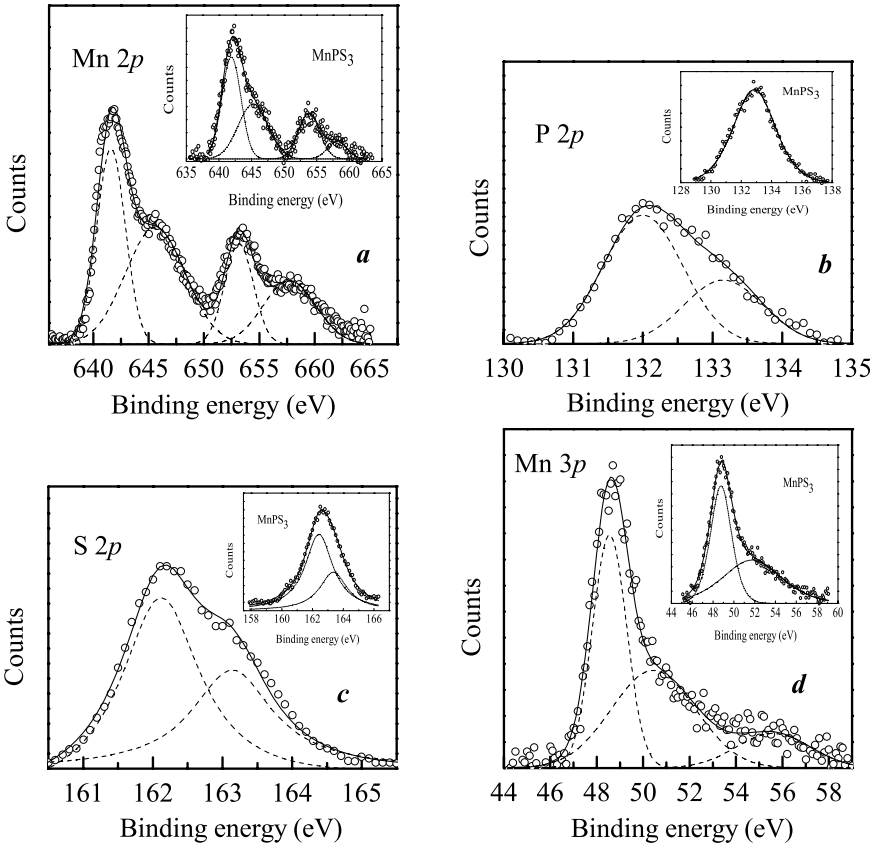

Fig. 8. – Mn $2p$ (a), P $2p$ (b), S $2p$ (c), Mn $3p$ (d), core-level XPS spectra in the $MnT_4/Li_{2x}Mn_{1-x}PS_3$ films; in the insets the corresponding XPS spectra in $MnPS_3$ are reported for comparison.

interacts with the exfoliated manganese thiophosphate the XPS signal of the Mn $2p$ core level of the Mn(III) ion present in this porphyrin is not detectable being hidden by the strong signal due to the thiophosphate Mn(II) ion.

Figure 8 reports the comparison between the Mn $2p$, P $2p$, S $2p$ and Mn $3p$ core level XPS spectra in the $MnT_4/Li_{2x}Mn_{1-x}PS_3$ film and in $MnPS_3$. These latter are presented in the corresponding insets. On going from $MnPS_3$ to $MnT_4/Li_{2x}Mn_{1-x}PS_3$ film all the above cited XPS spectra move of about 0.3 eV towards lower binding energies. Such a lower binding energy rigid displacement of all structures of the exfoliated manganese thiophosphate suggests an anionic behaviour for the matrix $MnPS_3$. This effect can be explained by considering that during the ion exchange intercalation most lithium ions present in the interlamellar space (van der Waals gaps) have been taken away producing negatively charged $Mn_{1-x}PS_3$ sheets which attract electrostatically the MnT_4 porphyrin cations. This explanation is experimentally confirmed by the lack of the chlorine counterions in the $MnT_4/Li_{2x}Mn_{1-x}PS_3$ film. Indeed the inset of fig. 9 shows that in the MnT_4 film both the Cl^- anions associated with the four positively charged N-methyl-4-pyridyl groups and the Cl^- anion coordinated to the central Mn(III) ion exhibit $2p_{3/2}$-$2p_{1/2}$ spin-

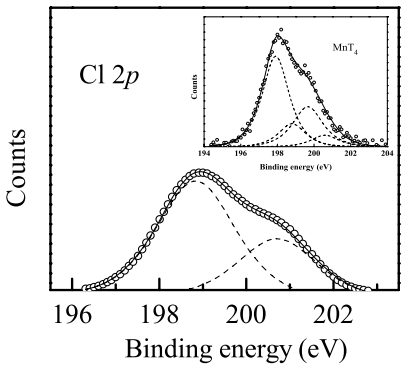

Fig. 9. – Cl $2p$ core-level XPS spectrum in the $MnT_4/Li_{2x}Mn_{1-z}PS_3$ film. The inset shows the XPS spectrum of the same level in the MnT_4 films.

orbit components positioned at 197.9 and 199.7 eV and at 198.8 and 200.7 eV (see table I), respectively, in an area ratio of 4:1. In the case of $MnT_4/Li_{2x}Mn_{1-x}PS_3$ film, only the axial chloride ligand is actually observed (see fig. 9) at the same binding energy position noted in the neat porphyrin film. In the Mn $3p$ core region XPS spectrum (see fig. $8d$) of the $MnT_4/Li_{2x}Mn_{1-x}PS_3$ film, in addition to the Mn $3p$ peak and its shake-up satellite at higher binding energy, a structure at about 55.6 eV is also visible. This feature, which is typical of Li^+ [20], can be mainly attributed to intralayer lithium ions. This could also justify why passing from the $Li_{2x}Mn_{1-x}PS_3$ film to the $MnT_4/Li_{2x}Mn_{1-x}PS_3$ film we observe a contraction in the basal spacing from 11.9 Å [17] to 11.0 Å as indicated by the XRD spectra. The presence of shake-up type satellites on the high binding energy side of the Mn $2p$ and $3p$ peaks (see fig.$8a$ and $8d$) suggests that in the $MnT_4/Li_{2x}Mn_{1-x}PS_3$ film the Mn-S bond is mostly ionic like in $MnPS_3$ [22, 23].

4. – Conclusion

X-ray photoemission and UV-Vis spectroscopies have given insight into the optical and electronic properties of $MnT_4/Li_{2x}Mn_{1-x}PS_3$ and MnT_4 films. Our experimental findings suggest that the interaction between the MnT_4 porphyrin and the $MnPS_3$ matrix is electrostatic in origin. Indeed no charge transfer from the guest species (the tetracationic MnT_4 porphyrin) to the host lattice ($MnPS_3$) occurs. The effects of metal insertion in the H_2T_4 porphyrin are mainly evident in the N $1s$ core level XPS spectrum which consists of two peaks in an 1:1 area ratio, instead of three peaks. This level is really the most sensitive probe for describing changes in the charge distribution in these porphyrins.

REFERENCES

[1] Lagadic I., Lacroix P. G. and Clement R., *Chem. Mater.*, **9** (1997) 2004.
[2] Grasso V. and Silipigni L., *Riv. Nuovo Cimento*, **25**, No. 6 (2002) 1.
[3] Lacroix P. G., Clement R., Nakatami K., Zyss J. and Ledoux I., *Science*, **263** (1994) 658.
[4] Coradin T., Clement R., Lacroix P. G. and Nakatami K., *Chem. Mater.*, **8** (1993) 2153.

[5] Léaustic A., Sour A., Riviére E., Clément R., *C.R. Acad. Sci. Paris, Chem.*, **4** (2001) 91.
[6] Clément R., Lacroix P. G., O'Hare D. and Evans J. S. O., *Adv. Mater.*, **6** (1994) 794.
[7] Bérnard S., Léaustic A., Riviére E., Pei Y. and Clément R., *Chem. Mater.*, **13** (2001) 3709.
[8] Silipigni L., De Luca G., Quattrone T., Monsú Scolaro L., Salvato G. and Grasso V., *J. Phys. Condens. Matter*, **18** (2006) 5759.
[9] Caseli L., Vinhado F.S., Iamamoto Y. and Zaniquelli M. E. D., *Colloids and Surfaces A: Physicochem. Eng. Aspects*, **229** (2003) 169;
[10] Gandini S. C. M., Borissevitch I. E., Perussi J. R., Imasato H. and Tabak M., *J. Lumin.*, **78** (1998) 53.
[11] Van Caemelbecke E., Kutner W. and Kadish K. M., *Inorg. Chem.*, **32** (1993) 438.
[12] Gandini S. C. M., Yushmanov V. E., Perussi J. R., Tabak M., Borissevitch I. E., *J. Inorg. Biochem.*, **73** (1999) 35.
[13] Bezerra A. G. Jr., Borissevitch I. E., de Araujo R. E., Gomes A. S. L. and de Araújo Cid B., *Chem. Phys. Lett.*, **318** (2000) 511.
[14] Li Z. and Xia C. G., *J. Mol. Cat. A: Chem.*, **214** (2004) 95.
[15] Chen F. C., Cheng S. H., Yu C. H., Liu M. H. and Su Y. O., *J. Electroanal. Chem.*, **474** (1999) 52.
[16] Purrello R., Monsú Scolaro L., Bellacchio E., Gurrieri S. and Romeo A., *Inorg. Chem.*, **37** (1998) 3647 and references therein.
[17] Silipigni L., Grasso V., De Luca G., Monsú Scolaro L. and Salvato G., *J. Appl. Phys.*, **98** (2005) 043307.
[18] Niwa Y., Kobayashi H. and Tsuchiya T., *J. Chem. Phys.*, **60** (1974) 799.
[19] Karweik D. H. and Winograd N., *Inorg. Chem.*, **15** (1976) 2336.
[20] Moulder J. F., Stickle W. F., Sobol P. E. and Bomben K. D., *Handbook of X-Ray Photoelectron Spectroscopy* (Perkin-Elmer Corporation) 1992.
[21] Piacentini M., Khumalo F. S., Olson C. G., Anderegg J. W. and Lynch D. W., *Chem. Phys.*, **65** (1982) 289.
[22] Grasso V., Santangelo S. and Piacentini M., *Solid State Ionics*, **20** (1986) 9.
[23] Grasso V., Neri F., Perillo P., Silipigni L. and Piacentini M., *Phys. Rev. B: Condens. Matter*, **44** (1991) 11060.